Unusual Photochemical C−N Bond Cleavage in the Novel Methyl 2-Chloro-3-methyl-2*H*-azirine-2-carboxylate

Andrea Gómez-Zavaglia,[†,‡] Agnieszka Kaczor,[†,§] Ana L. Cardoso,[†] Teresa M. V. D. Pinho e Melo,[†] and Rui Fausto*,[†]

Department of Chemistry, University of Coimbra, P-3004-535 Coimbra, Portugal, Faculdad de Farmacia y Bioquímica, Universidad de Buenos Aires, Junín 956, 1113 Buenos Aires, Argentina, and Faculty of Chemistry, Jagiellonian University, Ingardena 3, 30-060 Krakow, Poland

Received: April 4, 2006; In Final Form: May 9, 2006

The structure, preferred conformers, vibrational spectrum, and photochemical behavior of the novel azirine, methyl 2-chloro-3-methyl-2*H*-azirine-2-carboxylate (MCMAC) were investigated in low-temperature matrixes and in the neat solid amorphous state by infrared spectroscopy and quantum-chemical calculations. Two conformers of the compound were observed in argon, krypton, and xenon matrixes, in agreement with the DFT(B3LYP)/6-311++G(d,p) and MP2/6-311++G(d,p) theoretical calculations. Both conformers were found to exhibit the carboxylic ester group in the cis conformation, differing in the arrangement defined by the O=C−C−Cl dihedral angle (cis and trans, for Ct and Cc forms, respectively). The Ct conformer was found to be the most stable conformer in the gaseous phase as well as in both argon and krypton matrixes, whereas the more polar Cc conformer became the most stable form in the xenon matrix and in the neat solid amorphous phase. In situ broadband UV (λ > 235 nm) excitation of matrix-isolated MCMAC led to azirine ring C−C and C−N bond cleavages, the latter process corresponding to the most efficient reaction channel. The photochemical cleavage of the C−N bond had never been previously observed in the case of aliphatic 2*H*-azirines. Two electron withdrawing substituents (methoxycarbonyl group and chlorine atom) are connected to the azirine ring in the novel MCMAC azirine. The simultaneous presence of these two groups accelerates intersystem crossing toward the triplet state where cleavage of the C−N bond takes place. The primary photoproducts resulting from the C−N and C−C ring-opening reactions were also found to undergo further photochemical decarbonylation or decarboxylation reactions.

Introduction

2*H*-Azirines are unique strained molecules having a C=N bond incorporated into a three-membered ring. The ring system occurs naturally in some antibiotics such as azirinomycin, (isolated from *Streptomyces auras* cultures; **1** in Scheme 1) and its methyl ester.[1] In addition, both enantiomers of (*R*)−(+)- and (*S*)−(−)-dysidazirine **2** and (*S*)−(+)-antazirine **3** were isolated from the marine sponge *Dysidea fragilis*.[1]

Synthetically, 2*H*-azirines were first isolated in 1932 as intermediates in the reaction of oxime tosylates with base to give α-aminoketones.[2] Since 1953, when the structure of 2*H*-azirines was confirmed,[3,4] and mainly because of their high reactivity (both as nucleophiles and electrophiles), extensive research has been carried on the structure and reactivity, as well as thermo- and photochemical behavior of 2*H*-azirines.[5−15]

Azirines are important intermediates in the preparation of acyclic functionalized aminoderivatives and heterocycles.[16−18] In particular, 2*H*-azirines containing a carboxylic ester group, **4** (see Scheme 1), are excellent reagents for the preparation of functionalized aziridines[19] and α- and *β*-amino acid derivatives.[20−23]

The strategies of preparation of the above-mentioned derivatives might be variable, as the opening of the three-membered azirine ring might be accomplished owing to reactions with the proper reagents as well as from thermal or photochemical excitation. It has been reported that the C−N cleavage is generally favored by pyrolysis,[1,24−26] although C−C bond cleavage was also reported in the thermolysis of a series of 2-alkyl-3-phenyl substituted 2*H*-azirines.[27] On the other hand, photolysis of 2*H*-azirines has been shown to result almost invariably in ring-opening through heterolytic cleavage of the C−C bond, yielding nitrile ylides,[28] which can eventually react with 1,3-dipolarophiles to form the corresponding cyclic adducts (see Scheme 2).[28,29]

SCHEME 1: Relevant Naturally Occurring Azirines (1−3) and General Formula of 2*H*-Azirines Bearing a Carboxylic Ester Substituent at C2 (4)

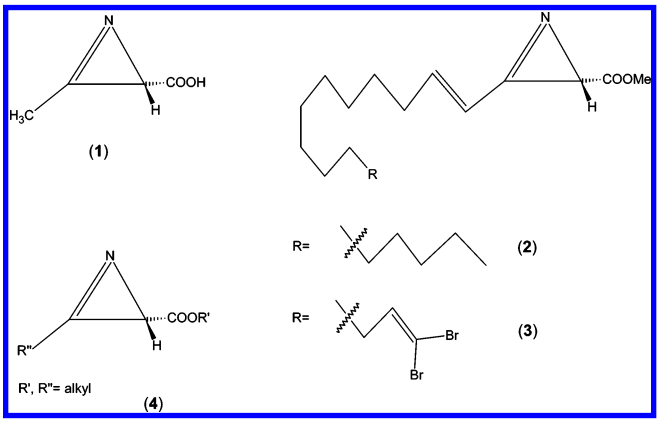

* To whom correspondence should be addressed. E-mail: rfausto@ci.uc.pt.
† University of Coimbra.
‡ Universidad de Buenos Aires.
§ Jagiellonian University.

10.1021/jp062094q CCC: $33.50 © 2006 American Chemical Society
Published on Web 06/13/2006

SCHEME 2: Photochemical C−C Bond Cleavage of 2*H*-Azirines and Subsequent Reaction of the 1,3-Dipole (Nitrile Ylide) with a 1,3-Dipolarophile (X = Y)

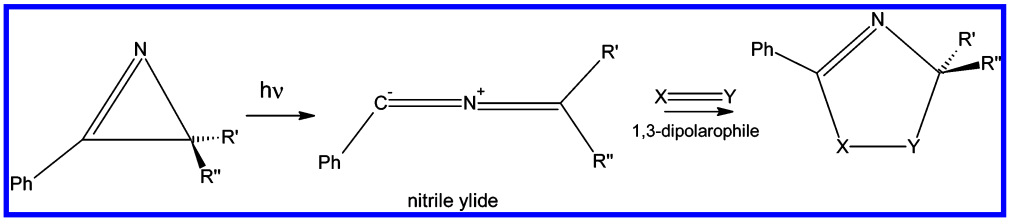

SCHEME 3: Synthetic Route to 2-Chloro-3-methyl-2*H*-azirine-2-carboxylate (MCMAC). The Product (7) Is Obtained as Racemic Mixture

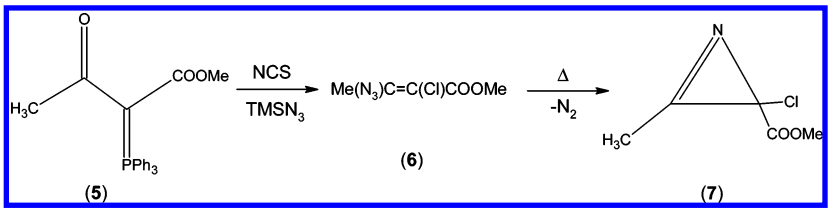

Quantum chemical theoretical studies gave further support to the reported mechanism of photochemical ring cleavage.[30−32] It has been suggested that a triplet intermediate is involved in the formation of the singlet nitrile ylide that follows opening of the ring by C−C bond cleavage.[30,33] More recently Klessinger and Borneman[34,35] concluded, in accordance with the observation of the ultrafast formation of phenylnitrile ylide from 2*H*-phenylazirine[36] that the photochemical process should occur from the nπ* S_1 excited state through a conical intersection between the S_1 and S_0 states.

The matrix isolation technique was also applied previously to the study of the photochemical cleavage of 2*H*-azirines. One of the main advantages of this method results from the fact that, in a matrix, the reactions are cage-confined. Since molecular diffusion is inhibited, no reactions involving species staying in different matrix sites will transpire, and only unimolecular reactions are expected which introduces a useful simplification in the study of photochemical reactivity. Very interestingly, it was Pimentel himself, the scientist that gave the name to the matrix isolation method,[37] who was the first to study photochemical reactions of 2*H*-azirines by matrix isolation spectroscopy.[38−40] Pimentel and co-workers were able to observe directly the nitrile ylides generated photochemically from 3-phenyl-2*H*-azirine as well as their isotopic labeled derivatives in N_2 matrixes at 12 K. Their detailed examination of the IR spectra revealed that the nitrile ylides do not have a propargyl-like structure, $C{\equiv}N^+{-}C^-$, but an allene structure with a slightly twisted $C^-{=}N^+{=}C$ moiety.[40]

Very recently, Inui and Murata[41−43] have demonstrated that both C−C and C−N bonds can indeed be cleaved upon photolysis of matrix isolated 2*H*-azirines bearing a naphthyl substituent on C2, depending on the irradiation wavelength. To explain the unusual photochemical cleavage of the C−N bond [which was achieved upon irradiation at long wavelength (>366 nm)], Inui and Murata[41−43] proposed a mechanism involving the formation of a vibrationally excited biradical with vinyl nitrene character. This species is generated from the triplet excited state of the azirine produced by the intersystem crossing from the S_1 state having an electronic character of a local $\pi-\pi^*$ excitation of the naphthyl moiety. This biradical later undergoes a Curtius-like rearrangement to the experimentally observed ketene imine. Very interestingly, the photochemical C−N bond cleavage has been found to be particularly sensitive to chemical substitution. Inui and Murata[41−43] reported that when 3-methyl-2-(1-naphthyl)-2*H*-azirine was irradiated with $300 < \lambda < 366$ nm light, the C−C cleavage occurred exclusively, whereas replacement of the naphthyl hydrogen in the para position relative to the 2*H*-azirine ring by a halogen atom produced a mixture of the products arising from the C−C and C−N bond cleavages, and its substitution by a NO_2 group led to the exclusive occurrence of the C−N bond cleavage.

Since, according to the previous reported studies,[41−43] the presence of electron withdrawing substituents on the azirine ring carbon atoms may favor the C−N photochemical cleavage, we decided to synthesize a novel 2*H*-azirine bearing the chloro and methoxycarbonyl substituents, methyl 2-chloro-3-methyl-2*H*-azirine-2-carboxylate (MCMAC) and study its photochemistry as an isolated species in cryogenic noble gas matrixes. This compound has also other structural characteristics that make it particularly interesting to be studied by the matrix isolation method: (a) It is a halo derivative (it is known that halo substituted azirines are highly unstable at room temperature; therefore, a cryogenic matrix offers an ideal environment for the study of their infrared spectra and monitoring their photochemistry). (b) It has a $COOCH_3$ substituent. This group has two main characteristics: it can react upon irradiation (e.g., in a decarboxylation or decarbonylation reaction), and it can give rise to conformational isomerism. (Two internal rotation axes can be associated with the $COOCH_3$ group: The first is associated with the C−C bond which connects the methoxycarbonyl moiety to the 2*H*-azirine ring, and the second is associated with the C−O bond allowing for the rotation of the OCH_3 group).

In the present study, a systematic search on the possible minima on the potential energy surface of the compound was performed at the density-functional theory (DFT) level to investigate the conformational preferences of MCMAC. Then, this information was used to aid the interpretation of the spectroscopic data obtained for the compound isolated in different noble gases (argon, krypton, and xenon) cryogenic matrixes. Finally, the reactivity of the matrix-isolated compound upon in situ UV broadband irradiation was investigated.

Materials and Methods

Synthesis and Characterization. MCMAC (**7**; Scheme 3) was prepared using a previously reported general synthetic route to 2-halo-2*H*-azirines.[44,45] The phosphorus ylide (**5**) (1.76 g, 4.5 mmol) was dissolved in dichloromethane (50 mL) and a solution of azidotrimethylsilane ($TMSN_3$; 0.71 g, 6.5 mmol) and *N*-

chlorosuccinimide (NCS; 0.87 g, 6.5 mmol) in dichloromethane (100 mL) was added. The reaction was completed after 5 min. The residue obtained upon removal of the solvent was purified by column chromatography [ethyl acetate−hexane (1:2)] and gave the methyl 3-azido-2-chlorobut-2-enoate (**6**) directly as a yellow oil (82%). A solution of the vinyl azide (2.0 mmol) in heptane (10 mL) was heated under reflux for 2.5 h (the reaction was monitored by TLC). The reaction mixture was cooled, and the solvent was evaporated giving the azirine (**7**) as a yellow oil (99%). ^{1}H NMR 2.62 (3H, s), 3.81 (3H, s); ^{13}C NMR 10.7, 53.2, 53.8, 165.6, 168.0; *m*/*z* (CI+) 166 (MNH_4^+, 100), 144 (30), 135 (25); HRMS (CI) *m*/*z* 148.0170 ($C_5H_7N_1O_2Cl$ [MH^+], 148.0165). Phosphorus ylide (**5**) was prepared using a general procedure described in ref 46.

Infrared Spectroscopy. The IR spectra were obtained using a Mattson (Infinity 60AR Series) Fourier transform infrared spectrometer, equipped with a deuterated triglycine sulfate (DTGS) detector and a Ge/KBr beam splitter, with 0.5 cm^{-1} spectral resolution. To avoid interference from atmospheric H_2O and CO_2, a stream of dry nitrogen was continuously purged through the optical path of the spectrometer. The compound was placed in a specially designed doubly thermostatable Knudsen cell, whose compartments (sample container and valve nozzle compartments) were kept at 298 K during deposition of the matrix. Matrixes were prepared by co-deposition of MCMAC vapors coming out of the Knudsen cell together with a large excess of the matrix gas (argon N60, krypton N48, or xenon N48; all obtained from Air Liquide) onto the CsI substrate of the cryostat cooled to 10 K (for argon and krypton matrixes) and 20 K (for xenon matrixes). All experiments were performed using an APD Cryogenics closed-cycle helium refrigeration system with a DE−202A expander. After depositing of the compound, annealing experiments were performed until a temperature of 35 K (Ar), 55 K (Kr), or 60 K (Xe) was attained.

Irradiation of the samples was carried out with a 150 W xenon arc lamp (Osram XBO 150W/CR OFR) or with the 500 W mercury(xenon) lamp (Newport, Oriel Instruments) through the outer KBr window of the cryostat (λ > 235 nm).

The low-temperature solid amorphous layer was prepared in the same way as the matrixes but with the flux of matrix gas cut off. The layer was then allowed to anneal at a slowly increasing temperature up to 215 K. IR spectra were collected during this process every 10−20 K of temperature change. After the temperature exceeded 215 K, the substrate was cooled back to 10 K, and spectra were collected each 10−20 K.

Computational Methodology. The quantum chemical calculations were performed with Gaussian 98[47] and Gaussian 03[48] at the MP2 and DFT levels of theory, with the standard 6-311++G(d,p) basis set. In the case of DFT calculations, the B3LYP density functional[49,50] was used. Geometrical parameters were optimized using the geometry direct inversion of the invariant subspace (GDIIS) method.[51,52] Vibrational frequencies were calculated at each level of theory and the nature of the stationary points on the potential energy surface (PES) resulting from optimization was determined by inspection of the corresponding calculated Hessian matrix. The optimized structures of all conformers described in this study were confirmed to correspond to true minimum energy conformations on the different potential energy surfaces investigated.

Potential energy profiles for internal rotation were calculated performing a relaxed scan on the DFT(B3LYP)/6-311++G(d,p) PES along the relevant reaction coordinates, and the transition state structures for conformational interconversion obtained using the synchronous transit-guided quasi-Newton (STQN) method.[53]

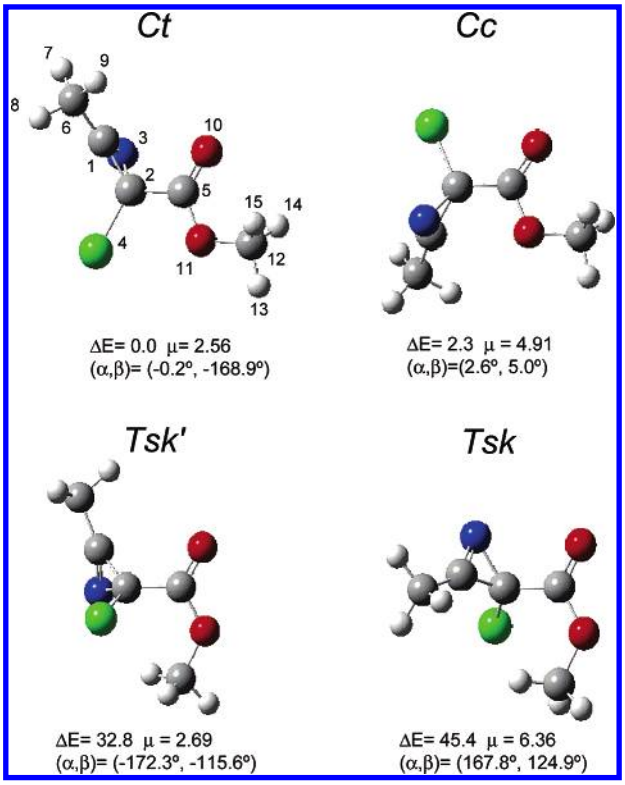

Figure 1. Conformers of MCMAC optimized at the DFT(B3LYP)/6-311++G(d,p) level of theory, with the atom numbering scheme. Relative energies (ΔE; in kJ mol^{-1}) and dipole moments (μ; in debye) are also provided, as well as the $O_{10}C_5O_{11}C_{12}$ (α) and $O_{10}C_5C_2Cl_4$ (β) dihedral angles (in degrees). The calculated energy of the most stable conformer (Ct) is −2256671.95 kJ mol^{-1}.

Normal coordinate analysis was undertaken in the internal coordinates space, as described by Schachtschneider,[54] using the program BALGA and the optimized geometries and harmonic force constants resulting from the DFT(B3LYP)/6-311++G(d,p) calculations.

Results and Discussion

Geometries and Energies. The MCMAC molecule can be understood as a chiral carbon atom bound to: (a) a $COOCH_3$ group; (b) a chlorine atom; (c) a $C(CH_3)$ group and (d) an azirinic nitrogen atom (see Scheme 3).

The molecule is characterized by two internal rotation axes, O=C−O−CH_3 and O=C−C−Cl, which can give rise to conformational isomers. To identify the minimum energy conformations of MCMAC, a systematic investigation of the potential energy surface of the molecule was undertaken using the B3LYP/6-311++G(d,p) method. Four different conformers were found (Ct, Cc, Tsk′, and Tsk; Figure 1), all of them belonging to the C_1 symmetry point group. The scheme adopted to designate the conformers is based on the conformations assumed by their relevant internal rotation axes: the conformation defined by the O=C−O−CH_3 dihedral angle is indicated by a capital letter (C = cis, 0°; T = trans, 180°), which is followed by lower case letters designating the conformation defined by the O=C−C−Cl dihedral angle (c = cis, 0°; t = trans, 180°; sk = skew, ca. 120°; sk′ = skew′, ca. −120°). The optimized geometries for the four conformers of MCMAC are provided in the Supporting Information (Table S1).

Table 1 displays the predicted relative energies (including zero-point energy corrections) of the conformers obtained at

TABLE 1: Calculated Relative Energies, Including Zero-Point Vibrational Contributions for the Conformers of MCMAC, Predicted Gas-Phase Conformer Abundances (T = 298 K), and Experimentally Determined Abundances in Different Matrices[a]

			population (298 K)[c]				
			calcd (%)		exptl (%)		
conformer	DFT(B3LYP)/ 6-311++G(d,p) ΔE_{ZPE}	MP2/ 6-311++G(d,p) ΔE_{ZPE}	DFT(B3LYP)/ 6-311++G(d,p)	MP2/ 6-311++G(d,p)	argon	krypton	xenon
Ct	0.0 (−2256671.95)[c]	0.0 (−2252334.42)[b]	71.7	66.4	68.1 ± 1.8	69.6 ± 2.4	63.1 ± 0.7
Cc	2.3	1.7	28.3	33.6	31.9 ± 1.8	30.4 ± 2.4	36.9 ± 0.7
Tsk′	32.8	34.0	0	0	0	0	0
Tsk	45.4	44.0	0	0	0	0	0

[a] Energies in kJ mol^{-1}; conformers are depicted in Figure 1. [b] Total energies with zero point vibrational energy contribution. [c] According to Boltzmann distribution.

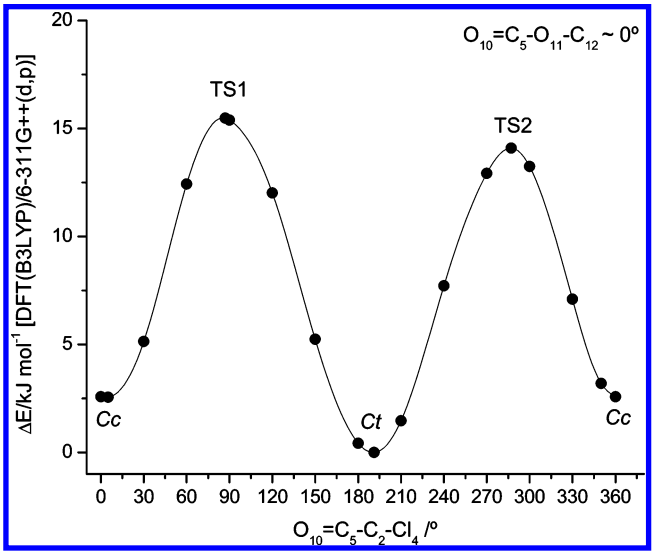

Figure 2. DFT(B3LYP)/6-311++G(d,p) calculated potential energy profile for conformational interconversion between Ct and Cc. TS1 and TS2 denote the two transitions states.

the B3LYP/6-311++G(d,p) and MP2/6-311++G(d,p) levels of theory. The calculations predict the Ct conformer as being slightly more stable than the Cc form (2.3 and 1.7 kJ mol^{-1} at the B3LYP and MP2 levels, respectively), while conformers Tsk′ and Tsk correspond to high-energy structures (ΔE > 30 kJ mol^{-1}) and are of no practical importance.

As it could be expected, the conformation within the methoxycarbonyl group (cis or trans) is the main factor determining the relative stability of the MCMAC conformers, whereas the conformation defined by the O═C−C−Cl dihedral angle appears only as a secondary factor. Indeed, the preference for the cis arrangement around the C−O bond has been found to constitute a very general rule for molecules bearing the carboxylic acid or carboxylic ester groups.[55−58] In MCMAC, the trans methoxycarbonyl conformation is further destabilized relative to the cis arrangement because in the former conformation strong steric repulsions between the methyl group and the chlorine atom exist. Accordingly, the O═C−C−Cl dihedral angle in both Tsk′ and Tsk is considerably different from 180°, contrary to what is observed in the two most stable conformers, where the O═C−C−Cl dihedral angle is close to 180° (see Figure 1).

The potential energy profile for interconversion between the two most stable conformers of MCMAC obtained at the B3LYP/6-311++G(d,p) level of theory is shown in Figure 2. Two transition states were found (TS1 and TS2), which are associated with the internal rotation around the C_2−C_5 bond in the two possible directions. Taking into account the low difference of energy between Cc and Ct (2.3 kJ mol^{-1}), the energy barriers for both the direct and reverse reactions are quite high (through TS1, 15.5 and 12.9 kJ mol^{-1}; through TS2, 14.1 and 11.5 kJ mol^{-1}, respectively). In the conformational studies of matrix isolated molecules, knowledge of the barriers to the intramolecular rotations is very important. More than 20 years ago Barnes[59] pointed out that the possibility of trapping a species in the matrix is related to the barrier to intramolecular rotation separating it from the lower energy species. According to the Barnes relation, barriers within the 12−15 kJ mol^{-1} range can be overcome at ca. 40−45 K.[59] This range of temperatures is too high to be useful for conformational studies performed in argon matrixes, because one expects that at 40 K the matrix is already considerably deteriorated and aggregation is already taking place extensively. However, in principle one can expect to be able to observe the Cc → Ct isomerization in both krypton and xenon matrixes, since these matrixes can be annealed to higher temperatures without significant matrix deterioration and molecular diffusion.

In summary, the theoretical results indicate that in the as-deposited matrixes observation of two conformers of MCMAC, Ct and Cc, might be expected. The relatively high energy barriers associated with the Cc → Ct conversion make this process unlikely to be observed upon annealing of argon matrixes. However, in both krypton and xenon matrixes, observation of the Cc → Ct conversion seems in principle to be possible by annealing the matrixes at temperatures above ca. 40 K.

Vibrational Spectra. *General Assignment.* MCMAC has 39 fundamental vibrations. For all the four conformers (Ct, Cc, Tsk′, and Tsk), all fundamental vibrations are predicted to be symmetry allowed in the infrared. Table S2 (Supporting Information) displays the definition of the internal coordinates used in the normal coordinates analysis undertaken in this study. The DFT(B3LYP)/6-311++G(d,p) calculated vibrational frequencies and infrared intensities for all the conformers of MCMAC (including the nonexperimentally observed Tsk′ and Tsk forms) and potential energy distributions (PEDs) of normal modes are given in Tables S3−S6 (Supporting Information).

Figure 3 depicts the as-deposited spectra of MCMAC in argon, krypton (T = 10 K), and xenon (T = 20 K) matrixes. The calculated spectra of the Ct and Cc forms (weighted by their estimated Boltzmann populations at 298 K: Ct, 72%; Cc, 28%) are also shown for comparison. Despite the systematic band splitting due to trapping of solute molecules in different matrix sites, the experimental spectra of MCMAC in all the three matrixes are well reproduced by the population-weighted calculated spectra of the two most stable conformers. This fact strongly facilitates the assignment of the experimental spectra, the proposed assignments being presented in Table 2.

Once the bands of a single conformer could be identified, it was possible to estimate the relative populations of the two conformers trapped in the different matrixes from the observed

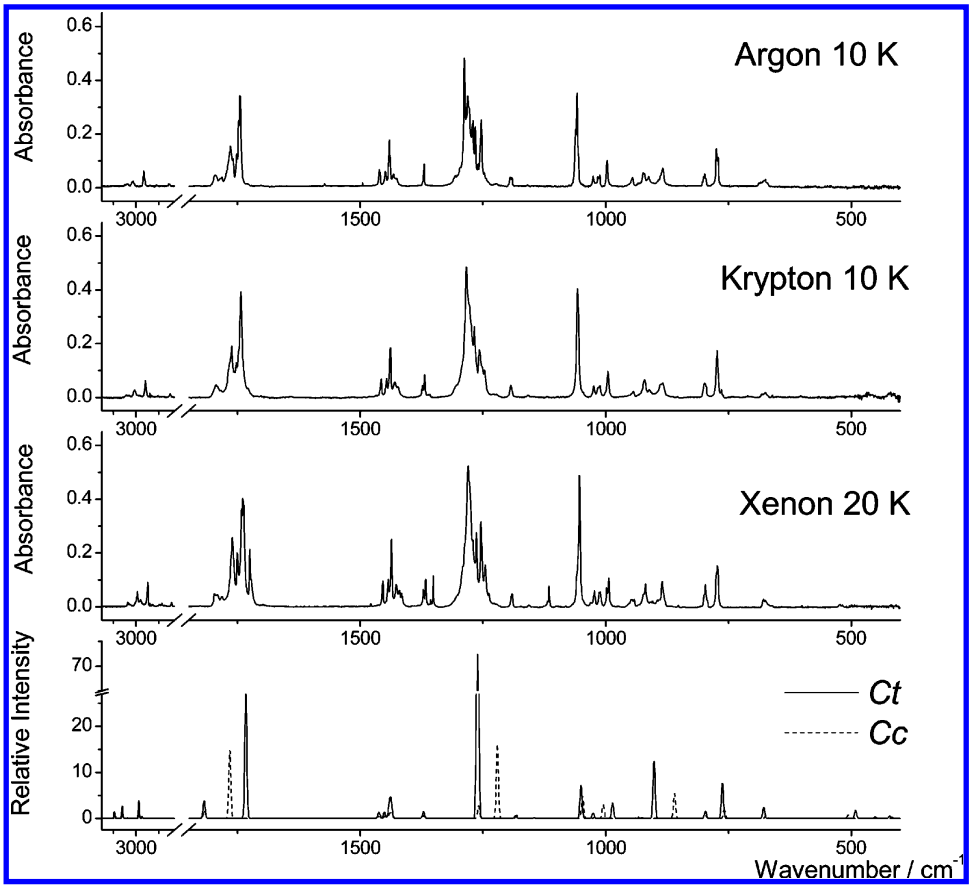

Figure 3. Infrared spectra of MCMAC isolated in solid argon, krypton, and xenon (as-deposited matrixes; substrate temperature: argon and krypton, 10 K; xenon, 20 K) and DFT(B3LYP)/6-311++G(d,p) theoretical spectra for Ct and Cc conformers scaled by their relative populations at 298 K (estimated from the calculated relative energies and assuming the Boltzmann distribution).

relative absorbances of bands associated with the individual forms, using the corresponding calculated infrared intensities as normalizing factors. In argon and krypton, the trapped populations of Ct and Cc conformers were found to be equal within the estimated experimental error (ca. 3%): 68 and 32% in argon, versus 70 and 30% in krypton. However, in xenon, the relative populations were found to be slightly different, with that of the Cc conformer increasing to 37% and the one of the Ct form decreasing to only 63%. This observation is in agreement with a relative stabilization of the more polar Cc conformer in the more polarizable xenon matrix (calculated dipole moments are 4.91 and 2.56 D for Cc and Ct, respectively). We shall return to this point in the next section.

Annealing Experiments. Annealing of the argon matrixes is limited by the relatively small temperature range that can be used without significant loss of matrix properties (less than ca. 40 K). The main spectroscopic changes observed upon annealing of the argon matrixes could be ascribed to conversion of less favorable to more favorable local environments. Indeed, noticeable changes in the relative intensities of the components of bands exhibiting multiplet structure because of matrix site splitting were observed. For instance, it is evident when the 1780−1710 cm^{-1} region is analyzed that, after annealing to 39 K, two (1752 and 1747 cm^{-1}) out of three bands attributed to the C═O stretching vibration of the Ct conformer reduce their intensity, whereas an increase in the intensity of the band at 1745 cm^{-1} is observed (Figure 4). Intensity changes in the bands assigned to the C═O stretching vibration of the Cc form are also noticed: the bands at 1771 and 1765 cm^{-1} reduce their intensity, with the simultaneous growth of their counterpart at 1759 cm^{-1}.

As mentioned before, use of the Barnes relation[59] predicts that the Cc → Ct conversion should not take place below 40 K. Hence, the nonobservance of any isomerization process in the argon matrix is consistent with the relatively high gas-phase energy barrier estimated for this process (>11 kJ mol^{-1}). On the other hand, aggregation became important at temperatures of ca. 25 K, with the appearance of characteristic bands of aggregates, for example, in the low-frequency range of the carbonyl stretching region (ca. 1733 and 1729 cm^{-1}), and because of the slight decrease of bands due to monomers. Apart from the diagnostic frequencies (lower than for both monomers) at which these bands appear, their behavior upon annealing is distinctive, as an increase in their intensity is observed not only at temperatures at which site-splitting effects are observed (i.e., relative changes in intensities of monomers' absorptions), but also at higher temperatures when a general decrease in the intensity of all bands due to monomers is observed. Annealing of a krypton matrix led to spectral changes identical to those observed in argon: extensive site-conversion followed, at higher temperatures, by aggregation. In this matrix, conformational isomerization could not be observed either.

Annealing of the xenon matrix yielded more interesting results. Below ca. 40 K, essentially site conversion was observed. Aggregation starts to become important at nearly this temperature. However, contrary to what was observed in argon and krypton matrixes, conformational isomerization could be observed in the xenon matrix. Very interestingly, it was the most stable conformer in the gaseous phase (Ct) that started to convert into the Cc form as soon as the temperature increased to 48 K. Such behavior can only be explained assuming that the relative order of stability of the two conformers is different in the gas

TABLE 2: Observed frequencies for the Ct and Cc conformers of MCMAC in argon, krypton, and xenon matrices and calculated frequencies and infrared intensities

Approximate Description [a]	Conformer	Calculated values DFT(B3LYP) /6-311++(d,p)		argon (10K)[b]		krypton (10K)[b]		xenon (20K)[b]		glassy state (10 K)	
		ν /cm^{-1} [c]	I / km mol^{-1} [d]	ν /cm^{-1}	I [e]	ν /cm^{-1}	I [e]	ν /cm^{-1}	I [e]	ν /cm^{-1}	I [e]
ν (OCH$_3$) as	*Ct*	3096	7.6	3038	vw	3042	vw	3036	vw	3033 [f]	w
ν (OCH$_3$) as	*Cc*	3092	3.2								
ν (OCH$_3$') as	*Ct*	3061	11.1	3015	vw	3007	vw	2994	vw	3005 [f]	w
ν (OCH$_3$') as	*Cc*	3060	4.3								
ν (CCH$_3$) as	*Ct*	3059	4.3								
ν (CCH$_3$) as	*Cc*	3058	1.6								
ν (CCH$_3$') as	*Ct*	3037	0.5					2980	vw	2981	w
ν (CCH$_3$') as	*Cc*	3036	0.3								
ν (OCH$_3$) s	*Ct*	2988	20.5	2967	w	2959	w	2949	w	2959	w
ν (OCH$_3$) s	*Cc*	2987	8.6							2929	w
ν (CCH$_3$) s	*Ct*	2974	2.4							2851	w
ν (CCH$_3$) s	*Cc*	2973	1.0								
ν C=N	*Ct*	1818	20.4	1795	w	1794	w	1797	w	1791	m
								1792	w		
ν C=N	*Cc*	1818	9.5	1784	vw			1781	vw		
ν C=O	*Cc*	1766	77.9	1771	m	1769[f]	m	1764[f]	s	1738	s
				1765	m	1762		1761	s		
				1759	m	1756	m	1759[f]	s		
ν C=O	*Ct*	1733	145.4	1752	m			1751	m		
				1747	s	1752	m	1744[f]	vs		
				1745	vs	1748[f]	s	1742	vs		
						1743	vs	1739	vs		
								1737	vs		
	(agg)[f]			1733	vw	1729	vw	1725	m		
	(agg)[f]			1729	vw			1722	w		
δ (OCH$_3$) as	*Ct*	1462	2.8	1461	w	1459[f]	w	1455[f]	w	1439	m
δ (OCH$_3$) as	*Cc*	1464	7.1	1460[f]	w	1457	w	1454	w		
δ (OCH$_3$') as	*Ct*	1451	7.3	1449	w	1447	w	1443	w		
δ (OCH$_3$') as	*Cc*	1450	2.6								
δ (CCH$_3$) as	*Cc*	1441	4.5	1443[f]	w	1439	m	1440	w		
δ (CCH$_3$) as	*Ct*	1441	11.3	1441	m			1436	m		
δ (OCH$_3$) s	*Ct*	1439	12.6	1432	w	1429	w	1427	w		
δ (OCH$_3$) s	*Cc*	1438	0.9								
δ (CCH$_3$') as	*Ct*	1437	11.7	1426	w	1423	w	1420	w		
δ (CCH$_3$') as	*Cc*	1436	4.9					1415	w		
δ (CCH$_3$) s	*Cc*	1371	3.4	1372[f]	w	1373	w	1372	w	1371	w
δ (CCH$_3$) s	*Ct*	1371	7.8	1370	m	1368	m	1367	m		
ν C-O	*Ct*	1261	309.7	1306	w	1305	w	1292[f]	m	1287	s
				1302	w			1287[f]	s		
				1296	w			1280	vs		
				1288	vs	1284	vs	1277[f]	s		
ν C-C$_\alpha$	*Ct*	1261	77.8	1281	s	1277[f]	s	1271	m		
				1279	s	1274[f]	s				
				1272	s						
				1271	s						
ν C-C$_\alpha$	*Cc*	1259	14.3	1266	s	1267	s	1263	s		
				1260	w						
ν C-O	*Cc*	1221	85.3	1256	m	1257	s	1254	s	1251[f]	w
				1254	s	1251	m	1245	m		
				1247	vw	1247	m	1238	w		
γ (OCH$_3$)	*Ct*	1184	3.0	1195	w	1193	w	1191	w	1194	w
γ (OCH$_3$)	*Cc*	1181	3.3	1193	w	1190[f]	w	1189[f]	w		
				1191	w						
γ (OCH$_3$')	*Ct*	1146	0.6			1158	wv			1156	w
γ (OCH$_3$')	*Cc*	1145	0.3								
ν C-C	*Ct*	1050	38.2	1061	s	1058	vs	1059[f]	m	1058	s
ν C-C	*Cc*	1047	25.5	1058	s			1054	s		
γ (CCH$_3$)	*Cc*	1023	1.1	1026	w	1024	w	1025[f]	w	1021	w
								1023	w		
γ (CCH$_3$)	*Ct*	1026	6.0	1016	w	1016	w	1014	w		
				1014	w						
				1012	w	1011	w	1011	w		
γ (CCH$_3$')	*Cc*	1005	15.7	999[f]	m	1001[f]	w	994?	w	1011	w
γ (CCH$_3$')	*Ct*	986	18.0	997	m	996	m	998?	w	996	w
ν C-CH$_3$	*Cc*	936	2.8	945	w	944	w	949	w	943	w
ν O-CH$_3$	*Ct*	926	0.8					946	w		
								944	w		
								942	w		
ν C-CH$_3$	*Ct*	901	66.2	923	w	920	w	923	w	921	w
				921	w			919	w		
				913	w	911	w	905	wv		
ν O-CH$_3$	*Cc*	860	28.4	888[f]	w	887[f]	m	895	vw	882	w
				884	m	884	m	885	w		
γ C=O	*Ct*	797	8.1	804[f]	vw	799	w	801[f]	vw	800	m
				799	w			797	w		
				796[f]	vw			793[f]	w		
γ C=O	*Cc*	796	3.0	801[f]	vw	795[f]	w	799[f]	vw		
δ O=C-O	*Ct*	762	40.7	775	m	773	m	775[f]	m	774	s
δ O=C-O	*Cc*	758	9.7	771	m	764	vw	773	m		
ν C-N	*Ct*	678	12.6	675	vw	677	vw	678	vw	680	w
ν C-N	*Cc*	673	4.3	675	vw			675	vw		

[a] See Table S1 (Supporting Information) for definition of coordinates: ν, bond stretching; δ, bending; γ, rocking; τ, torsion; w, wagging; tw, twisting; s, symmetric; as, asymmetric. [b] Multiple trapping sites are grouped with parenthesis. [c] Scale factors = 0.978, [d] Intensities were weighted by the population factor (T = 298 K) for each conformer. [e] s, strong; w, weak; vw, very weak; vs, very strong; m, medium. [f] Shoulder. [g] agg denotes aggregate.

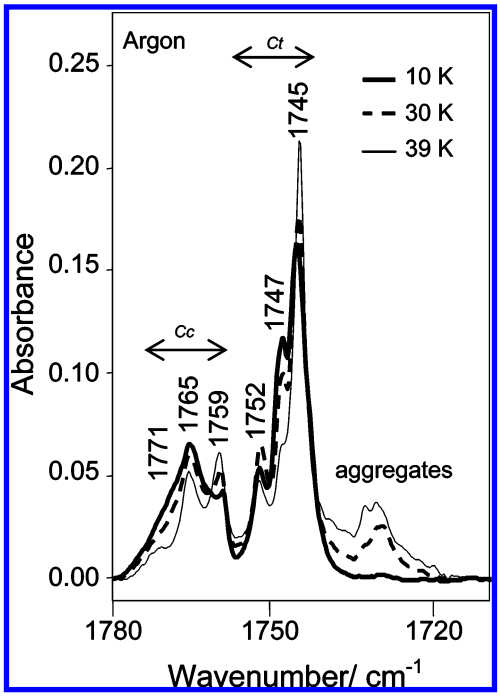

Figure 4. Carbonyl stretching region of the infrared spectra of MCMAC trapped in argon matrix, obtained immediately after deposition and after annealing at 30 and 39 K.

phase (where Ct is the most stable form) and in a xenon matrix (where Cc becomes the conformational ground state). Indeed, as already mentioned, Cc is certainly stabilized in the xenon matrix, because of its significantly higher dipole moment compared to the Ct form (4.91 vs 2.56 D). As it can be concluded from the annealing experiments in the xenon matrix, this stabilization is large enough to overcome the ca. 2 kJ mol^{-1} Cc−Ct energy difference predicted by the calculations for the gas phase. The phenomenon of stabilization of more polar conformers in more polarizable matrixes (as the xenon matrix) is well described in the literature.[60−63] Moreover, the change of order of relative stability of Cc and Ct is also in agreement with the above-mentioned observation that the relative population of the Cc conformer was found to be larger in the as-deposited xenon matrix when compared with both argon and krypton matrixes. Indeed, these results indicate that in the case of xenon, conformational cooling can partially occur during deposition of the matrix, leading to an increase of the population of the most stable conformer in the matrix, Cc, in the as-deposited xenon matrix relative to the gas phase. On the other hand, for both argon and krypton matrixes, conformational cooling during deposition (if it occurs) would increase the population of the Ct conformer, because in these matrixes the Ct conformer, like in the gaseous phase, is the most stable form. It is, however, well known that conformational cooling is significantly more efficient in xenon than in krypton or argon matrixes.[61,62]

The useful spectral regions to observe these changes correspond to the 1810−1710 and 1330−1210 cm^{-1} ranges (Figure 5). As described above, the increase of the temperature of the matrix up to 48 K produces stabilization of some matrix sites and, simultaneously, aggregation but *not* conformational changes. Therefore, in the carbonyl stretching region a counterpart of the ν(C═O) of the Ct conformer at 1737 cm^{-1} grows at the expense of two higher-frequency components at 1742 and 1739 cm^{-1}; similar behavior is observed for the ν(C═O) of conformer Cc (bands at 1764 and 1759 cm^{-1} increase in intensity at expenses of the band at 1761 cm^{-1}). These changes closely

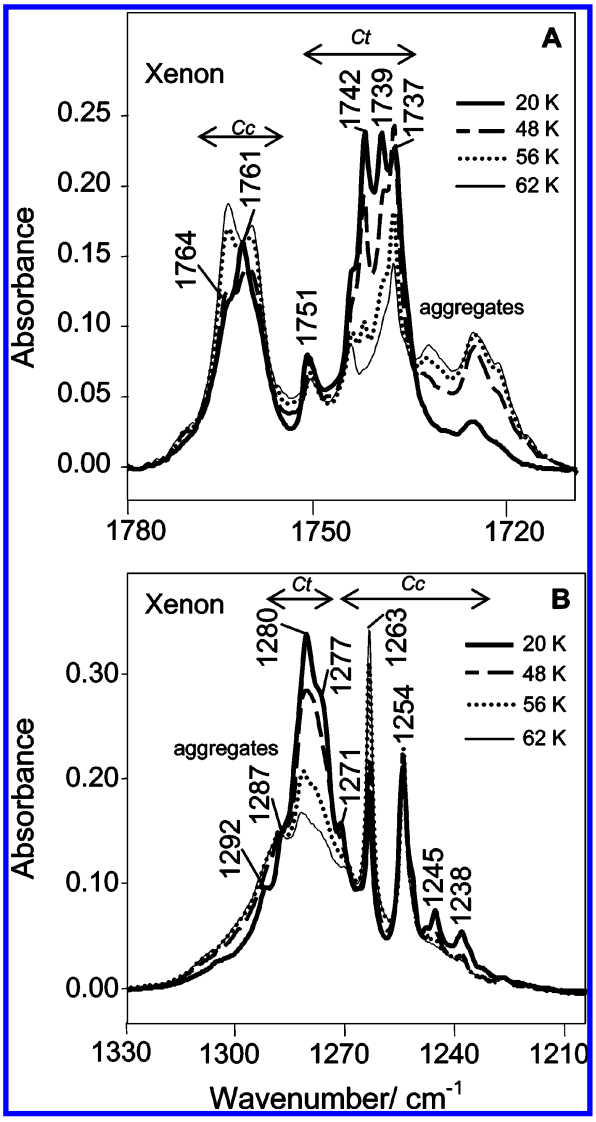

Figure 5. Carbonyl stretching region (top) and νC−O and νC−C$_\alpha$ stretching region (bottom) of the infrared spectra of MCMAC trapped in xenon matrix, obtained immediately after deposition and after annealing at 48, 56, and 62 K.

resemble the behavior of the analogous absorptions in the argon matrix (see Figure 4). In addition, both ν(C═O) groups of bands treated as a whole decrease in intensity because of the formation of aggregates (as noticed by the appearance of the aggregates' characteristic absorptions at 1725 and 1722 cm^{-1}). However, above 48 K, the occurrence of an additional parallel process (Ct → Cc conformational conversion) is noticeable. The significant increase of the group of bands due to ν(C═O) in the Cc conformer over their original abundance concomitant with the decrease of all counterparts associated with ν(C═O) in the Ct conformer is the experimental proof of this process (see Figure 5A).

In the 1330−1210 cm^{-1} region (Figure 5B), the absorption at 1263 cm^{-1}, associated with the ν(C−O) mode of the Cc conformer, increases systematically in intensity upon annealing: first because of site changes, at the expense of decrease in intensity of the band at 1271 cm^{-1} (which is also due to Cc), and then, above 48 K, because of both site conversion and the Ct → Cc isomerization. Concomitantly, the decrease of the whole group of bands associated with ν(C−O) in the Ct conformer (at 1292, 1287, 1280, and 1277 cm^{-1}) is clearly observable.

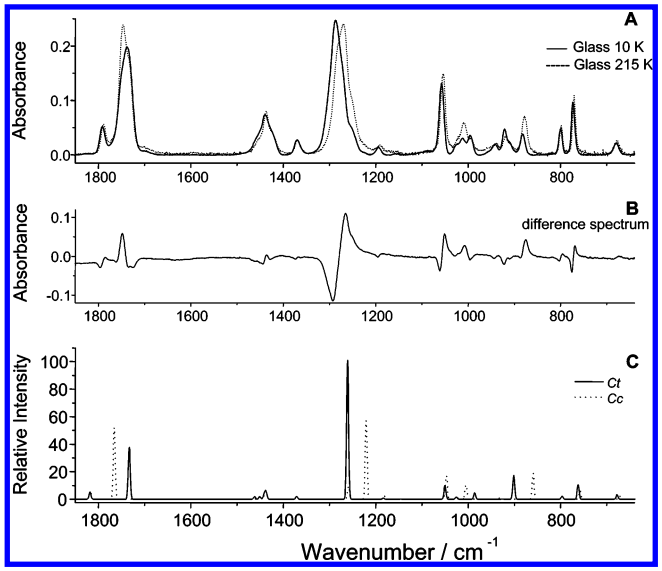

Figure 6. (A) Infrared spectra of MCMAC in the glassy state (see the Materials and Methods section for a detailed description of the experimental conditions) at 10 and 215 K; (B) difference spectrum (215 − 10 K); (C) infrared calculated spectra for Ct and Cc conformers of MCMAC.

In summary, in xenon matrixes, annealing above 48 K leads to an increase in intensity of the bands associated with aggregates, which occurs at the expense of a decrease in the intensity of all bands corresponding to the Ct form. Simultaneously, the bands associated with the most stable matrix sites of the Cc conformer increase in intensity because of the simultaneous occurrence of Ct → Cc isomerization.

Spectra of the Low-temperature Neat Amorphous Layer. The analysis of the spectra obtained for MCMAC in the glassy state produced by fast deposition of the vapor of the compound at 298 K onto the coldfinger of the cryostat at 10 K (Figure 6) revealed that the most stable conformer of the compound in the neat low-temperature amorphous solid is, as for the compound isolated in the xenon matrix, the more polar Cc form. The experimental data shown in Figure 6 correspond to the spectra obtained immediately after preparation of the amorphous film of the neat compound and after annealing the sample at 215 K (panel A). The difference spectrum (215 − 10 K; panel B) and the calculated spectra for the two conformers, Ct and Cc, (panel C) are also given for comparison. From this figure, it can be easily concluded that the Ct → Cc conversion takes place during the annealing, since the bands due to conformer Cc increase their intensity at the expense of those that originated in conformer Ct. These results unequivocally express the higher stability of the Cc conformer in this phase, since the as-deposited amorphous layer resulting from fast deposition of the compound onto the cold substrate of the cryostat essentially preserves the conformational equilibrium existing in the gas phase prior to deposition and then relaxes to a less energetic state upon annealing by converting Ct molecules (less stable in this phase) into the most stable C*c* molecules.

Photochemistry (UV Irradiation Experiments; λ > 235 nm). *Identification of Photoproducts and Reaction Paths.* Upon broadband UV irradiation (λ > 235 nm) of matrix-isolated monomeric MCMAC, the original bands of the compound lost intensity while new bands were formed. The most prominent features of the photoproducts were observed in the 2150−2050 cm^{-1} spectral range. Table S7 presents the band assignments for the main photolysis products of MCMAC. The proposed reaction pathways are schematically shown in Figure 7. Figures 8 and 9 show selected spectral ranges where the features due to the photoproducts are observed and which were particularly useful to the interpretation of the experimental results presented below.

According to the spectroscopic observations, photolysis of matrix-isolated MCMAC follows two different reaction pathways (see Figure 7): (i) it can undergo the usual azirine ring C−C bond cleavage, giving the nitrile ylide [(1-chloro-2-methoxy-2-oxoethylidene)iminio] ethanide (thorough this paper referred to as P1), or (ii) it can suffer the C−N bond cleavage, to yield methyl 2-chloro-3-(methylimino)acrylate (P2). Very interestingly, it is this last reaction, which, as mentioned in the

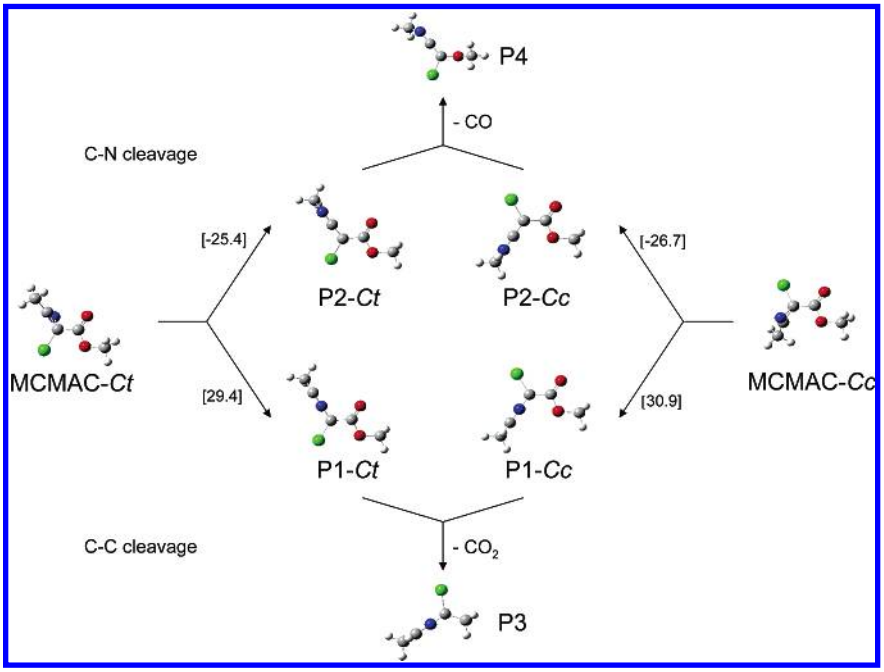

Figure 7. Proposed reaction pathways resulting from irradiation of MCMAC through the outer KBr window of the cryostat (λ > 235 nm). Zero-point corrected energies (in kJ mol^{-1}) of primary photoproducts (P1 and P2) relative to the relevant reactant conformer of MCMAC are given in brackets. Secondary photoproducts, P3 and P4, were only observed when irradiation was carried out with the 500 W Hg(Xe) source.

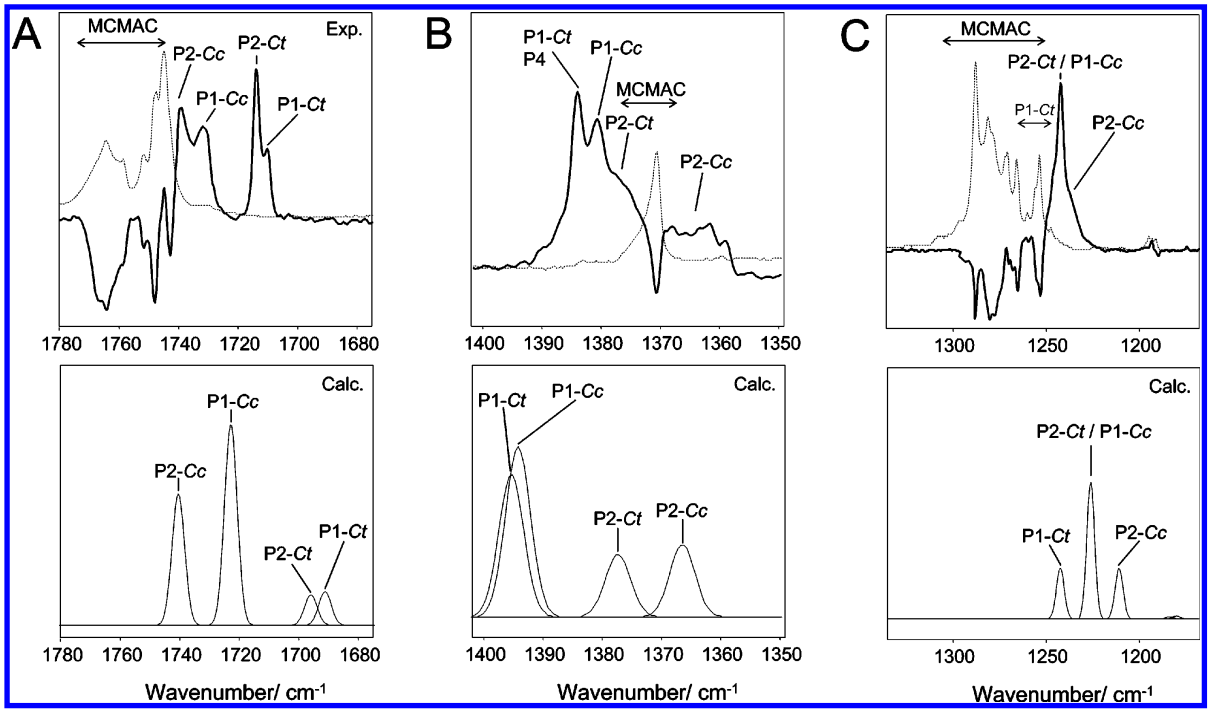

Figure 9. Changes in infrared spectrum of MCMAC by UV (λ > 235 nm) irradiation of the argon matrix with the 500 W Hg(Xe) lamp along with the B3LYP/6-311++G(d,p) calculated spectra of the observed photoproducts. The calculated bands were simulated using Gaussian functions centered at the scaled frequency (scale factor: 0.978) and with the bandwidth at half-height equal to 5 cm^{-1}: (A) 1780−1680 cm^{-1} range; (B) 1400−1350 cm^{-1} range; (C) 1330−1170 cm^{-1} range.

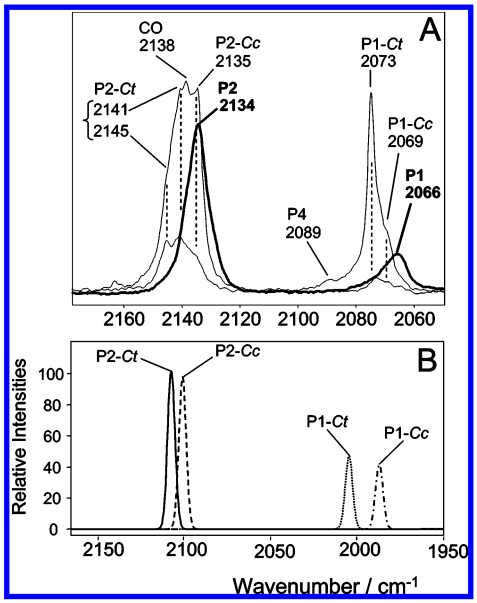

Figure 8. (A) Changes in infrared spectrum of MCMAC by UV (λ > 235 nm) irradiation in the 2180−2050 cm^{-1} region. The thick line corresponds to the spectrum obtained in the xenon matrix, after 7.5 h of irradiation with the 150 W Xe lamp. The thin lines correspond to spectra obtained in the argon matrix: the lower intensity spectrum after irradiation during 22.8 h with the 150 W Xe lamp, the higher intensity spectrum after 10 min of irradiation with the 500 W Hg(Xe) source. (B) B3LYP/6-311++G(d,p) calculated spectra of P1 and P2 in the relevant spectral region. The calculated bands were simulated using Gaussian functions centered at the calculated scaled frequency (scale factor: 0.978) and with the bandwidth at half-height equal to 5 cm^{-1}.

Introduction section, is a very unusual photochemical process in azirines, that corresponds to the preferred route, as shown in detail later in this paper.

Both P1 and P2 can exist in two different low energy conformers (see Figure 7), which have the methoxycarbonyl group in the cis conformation and differ in the conformation defined by the O═C−C−Cl dihedral angle. Such conformers can be correlated with the two low energy forms of MCMAC and will be designated as Pn-Cc and Pn-Ct, where n = 1 or 2.

After irradiation of MCMAC isolated in argon matrix with the Xe lamp, the most intense bands of the photoproducts occur at 2145/2141 and 2135 cm^{-1} (Figure 8). These bands were assigned to the ν(C═C═N) asymmetric stretching mode in the two conformers of P2, P2-Ct (2145/2141 cm^{-1}), and P2-Cc (2135 cm^{-1}), which result from the C−N bond cleavage of the azirine ring of Ct and Cc conformers of MCMAC, respectively. In the xenon matrix, the bands due to the two conformers of P2 are extensively overlapped and give rise to the band with maximum at 2134 cm^{-1} (Figure 8). A second set of intense bands due to a photoproduct appears at lower frequencies, 2073 and 2069 cm^{-1} (with a counterpart in the asymmetric band at 2066 cm^{-1} in the xenon matrix). These bands were assigned to the ν(C^{-}═N^{+}═C) vibration of P1-Ct and P1-Cc conformers, respectively, resulting from the C−C bond cleavage of the azirine ring in the two MCMAC conformers.

Besides these bands, additional bands of P1 and P2 that are predicted by the calculations to be intense could also be observed in other regions of the spectra of the irradiated matrixes. Figure 9 presents selected regions of a difference spectrum obtained by subtraction of the spectrum of as-deposited argon matrix from the spectrum of the irradiated sample. In all three selected regions shown in the picture, positive absorptions are observed, which are ascribable either to P1 or P2. In the 1780−1680 cm^{-1} range (Figure 9A), four new bands appeared at 1738 (P2-Cc), 1732 (P1-Cc), 1714 (P2-Ct), and 1710 (P1-Ct) cm^{-1}, which are due to the νC═O stretching vibrations of the P1 and P2 conformers. In the 1400−1350 cm^{-1} range (Figure 9B), the P2 conformers are predicted to give rise to bands at lower frequencies than P1; accordingly, bands due to P2-Ct and P2-Cc are observed at ca. 1372 and 1363 cm^{-1}, respectively, while those due to P1-Ct and P1-Cc are observed at 1383 and 1380 cm^{-1}. Finally, in the 1330−1130 cm^{-1} range (Figure 9C), the

band at 1243 cm^{-1} is attributed to both P2-Ct and P1-Cc and the shoulder at 1237 cm^{-1} to P2-Cc; P1-Ct is expected to absorb at a slightly higher frequency and it is certainly buried within the features due to MCMAC in the 1300−1250 cm^{-1} range.

The formation of carbon dioxide (characteristic bands in the 2350−2335 cm^{-1} range) was observed in all irradiation experiments. All possible secondary products of decarboxylation of P1 and P2 were investigated theoretically, suggesting that [(1-chloroethylidene)iminio]ethanide ($CH_3CClNCCH_3$; P3) is formed in result of a secondary reaction of P1. The two most intense absorptions of P3 are observed at 1853 (Ar) and 1848 (Xe) cm^{-1} (calc: 1883 cm^{-1}) and at approximately 1001 (Ar) and 1003 cm^{-1} (Xe) (calc: 1090 cm^{-1}).

When the argon matrix was irradiated with the more efficient Hg(Xe) lamp, an additional band was observed at 2138 cm^{-1}, overlapped with the previously diagnosed bands [at 2145, 2141 (shoulder in this case), and 2135 cm^{-1}] (Figure 8). The 2138 cm^{-1} band can be doubtlessly assigned to carbon monoxide.[64] Besides, several new low intensity bands emerging in other spectral regions (including the small band observed at 2089 cm^{-1}, which can be seen in the data shown in Figure 8) were also observed in the spectrum of the irradiated [by Hg(Xe)] matrix. The appearance of all these new bands is a clear indication that upon irradiation with the Hg(Xe) lamp, the primary photoproducts undergo further photochemical reactions, which implies extrusion of CO. Therefore, the vibrational spectra of all potential products of degradation of P1 and P2 resulting from extrusion of CO were calculated theoretically and compared with the experimental data. *N*-(2-chloro)-2-methoxyethenylidene methanamine ($CH_3OCClNCCH_3$; P4), with most intense bands at 2089 cm^{-1} (calc: 2088 cm^{-1}), ca. 1499 cm^{-1} (calc: 1464 cm^{-1}), 1383/1380 cm^{-1} (calc: 1368 cm^{-1}), and 1075 cm^{-1} (calc: 1062 cm^{-1}) is the proposed product of decarbonylation of P2.

The assignment of P3 and P4 products should be treated as tentative because of the quite low efficiency of the observed secondary reactions and the extensive overlap of bands due to these compounds with absorptions of other species, namely P1 and P2. Nevertheless, the highest intensity bands of P3 and P4 predicted by calculations fit fairly well the newly formed bands, as it was shown above. For a full listing of calculated vibrational frequencies for all identified products of photolysis of MCMAC, please refer to Tables S8−S10 (Supporting Information).

Relative Efficiency of C−N and C−C Azirine Ring Photocleavages. To evaluate which of the two pathways occurs preferentially, the integral intensity of the intense bands due to the νC=C=N (P2) and $\nu C^{-}=N^{+}=C$ (P1) asymmetric stretching modes (normalized by the corresponding calculated intensity) were plotted against the time of irradiation (Figure 10). The evaluation was done only for results of irradiation with the Xe lamp because, as mentioned above, under Hg(Xe) lamp excitation, bands due to other than the primary photoproducts P1 and P2 appeared in the investigated spectral region overlapping the absorptions of the relevant species. A P2/P1 ratio between the normalized intensities of approximately 2 was obtained in both argon and xenon matrixes, indicating that, very interestingly, the C−N azirine ring cleavage in MCMAC is preferred over the C−C bond breakage. (It shall be noticed that the P2/P1 intensity ratio is certainly somewhat affected by the fact that P1 partially reacts to give rise to P3. However, the extension of this last process is quite low, and it can be neglected in practical terms.)

According to our knowledge, the photochemical cleavage of the C−N bond was not observed, up to now, in the case of aliphatic 2*H*-azirines. The cleavage of this bond in aromatic compounds was explained as a result of aromatic $\pi \rightarrow \pi^*$ transitions (of lower energy than n $\rightarrow \pi^*$) and the subsequent intersystem crossing to a triplet intermediate.[34,41−43] Upon the lack of aromatic rings in MCMAC, other factors have to be responsible for the observed prevalence of the C−N bond cleavage over the in general more common C−C bond cleavage. As mentioned in the Introduction, Inui et al.[41] demonstrated that in 1-naphthyl substituted azirines, the substitution of the naphthyl hydrogen in para position with respect to the 2*H*-azirine aromatic ring by a Br atom increased the efficiency of the C−N cleavage compared to C−C. This phenomenon may be explained assuming that substitution by the halogen accelerates intersystem crossing and stabilizes the triplet state,[41] thus leading to the preferred formation of the ketene imine (P2, in our case). On the other hand, the reaction of photoproduction of the nitrile ylide (P1 in our case) proceeds via singlet state, and it is barrierless.[35] Additionally, it was also shown that in this last case, the reverse reaction (reformation of the 2*H*-azirine from the nitrile ylide) takes place upon irradiation[38−41] as well; this is in consonance with the very low barrier for this reaction predicted by CASPT2 computations (11 kcal mol^{-1} for 2*H*-azirine).[35]

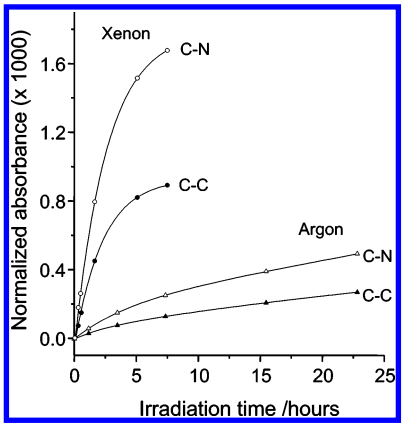

Figure 10. Change with time of irradiation (with Xe lamp) of the integral intensity of the characteristic bands of MCMAC main photoproducts, P1 (2090−2060 cm^{-1}) and P2 (2150−2120 cm^{-1}). All spectra used to obtain the points in the graphic were first normalized in such a way that the initial amount of the reactant in both matrixes was equal. For each photoproduct, the bands were then renormalized by the DFT-(B3LYP)/6-311++G(d,p) calculated intensities (average value of Ct and Cc conformers; see Table S7). The formation of P1 and P2 correlates with azirine ring C−C and C−N cleavage, respectively (see text for detailed discussion).

In the described irradiation experiments, excitation of MCMAC to its lowest S_1 state shall then take place (leading to the C−C cleavage) followed by intersystem crossing to the lower in energy triplet state (leading to the C−N cleavage). Intersystem crossing is accelerated because of the presence of the electron withdrawing substituents (methoxycarbonyl group and chlorine atom) in the molecule, leading to a more efficient C−N cleavage compared to the C−C. Additionally, the simultaneous reformation of MCMAC in the matrix from P1 may also take place, while the cleavage of the C−N bond is, with all probability, an irreversible process. [The calculated relative energies of the photoproducts support this proposition. In fact, both conformers of P2 are ∼30 kJ mol^{-1} *lower* in energy than MCMAC, whereas P1 conformers have energies ∼30 kJ mol^{-1} *higher* than the reactant species (see Figure 7).] This also contributes to increase the relative efficiency of the C−N bond breaking process in MCMAC compared to the C−C cleavage.

Finally, since in general xenon matrixes privilege photochemical reactions that occur through a triplet state,[65,66] the amounts of P1 and P2 formed upon irradiation of the argon and xenon matrixes were compared in order to evaluate the influence of the matrix gas on the relative preference of the two observed photolysis channels. The similar product ratios observed in the different matrix gases indicate that in the case of MCMAC the properties of the matrix gas do not contribute decisively to determine the *relative* efficiency of the two reaction channels, both being favored in xenon compared to argon in a similar way. It can then be concluded that, in the line of the indications provided by previous studies on the other 2-substituted azirines,[41−43] the presence of the electron withdrawing substituents (chorine and methoxycarbonyl) on the azirine ring of MCMAC assumes the main role in determining the observed preference for the C−N bond photocleavage pathway over the generally preferred in azirines C−C photocleavage.

Conclusions

The structure, preferred conformers, vibrational spectrum, and photochemical behavior of the novel azirine, methyl 2-chloro-3-methyl-2*H*-azirine-2-carboxylate (MCMAC) were investigated in low-temperature matrixes and neat solid amorphous state by infrared spectroscopy and quantum-chemical calculations. Two conformers of the compound were observed in the argon, krypton, and xenon matrixes, in agreement with the B3LYP and MP2 theoretical calculations. Both conformers were found to exhibit the carboxylic ester group in the cis conformation, while they differ by the arrangement defined by the O═C−C−Cl dihedral angle (cis and trans, for Ct and Cc forms, respectively). The Ct conformer was found to be the most stable conformer in the gaseous phase as well as in both argon and krypton matrixes. However, the comparable energy of both conformers [$\Delta E_{(Cc-Ct)} = 2.3$ and 1.7 kJ mol^{-1} as calculated at B3LYP/6-311++G(d,p) and MP2/6-311++G(d,p) levels of theory, respectively, for the isolated molecule in a vacuum] along with the significantly higher dipole moment of the Cc form (4.91 vs 2.56 D for Ct) resulted in the increased stabilization of this conformer, which becomes the most stable form in the xenon matrix, as well as in the neat compound in the solid amorphous phase.

Broadband UV ($\lambda > 235$ nm) excitation of MCMAC brought photoisomerization of the compound as primary photoreactions, leading to production of [(1-chloro-2-methoxy-2-oxoethylidene)-iminio] ethanide (P1) and methyl 2-chloro-3-(methylimino)-acrylate (P2), obtained via the azirine ring C−C or C−N bond cleavage, respectively. The latter process was shown to correspond to the most efficient reaction channel.

The photochemical cleavage of the C−N bond had never been observed for aliphatic 2*H*-azirines, and even in the case of aromatic 2*H*-azirines, where it has already been reported to take place,[41−43] it was in general observed as a nonpreferential process (with C−C bond cleavage being the preferred reaction channel). The simultaneous presence in the novel azirine here studied of two electron withdrawing substituents connected to the azirine ring (methoxycarbonyl group and chlorine atom) accelerates intersystem crossing toward the triplet state that leads to irreversible cleavage of the C−N bond, which then becomes preferred over the reversible break of the C−C bond.

Under further irradiation, the primary photoproducts, P1 and P2, were found to undergo subsequent photochemical transformations, with *N*-(2-chloro)-2-methoxyethenylidene methanamine (P4), resulting from decarbonylation of P2, and [(1-chloroethylidene)iminio]ethanide (P3), created as a result of decarboxylation of being the most probable products.

Acknowledgment. This work was funded by Fundação para a Ciência e a Tecnologia, Portugal (Grant #SFRH/BPD/17081/2004) and projects POCTI/QUI/59019/2004, POCTI/QUI/58937/2004, SeCyT-GRICES: PO/PA04-EVI/001 and PO/PA04-EIX/018, FEDER, and Agencia Nacional de Promoción Científica y Tecnológica (PICT 13080). A.G.Z. is member of the Research Career of the Consejo Nacional de Investigaciones Científicas y Técnicas (CONICET, Argentina). Calculations were partially done at the Academic Computer Center "Cyfronet", Krakow, Poland (Grant KBN/SGI_ORIGIN_2000/UJ/044/1999), which is acknowledged for computing time.

Supporting Information Available: Tables of calculated frequencies, intensities, and energies and definitions of internal coordinates in pdf format. This material is available free of charge via the Internet at http://pubs.acs.org.

References and Notes

(1) Pinho e Melo, T. M. V. D.; Rocha Gonsalves, A. M. d'A. *Curr. Org. Synth.* 2004, *1*, 275.
(2) Neber, P. W.; Burghard, A. *Justus Liebigs Ann. Chem.* **1932**, *493*, 281.
(3) Cram, D. J.; Hatch, M. J. *J. Am. Chem. Soc.* **1953**, *75*, 33.
(4) Hatch, M. J.; Cram, D. J. *J. Am. Chem. Soc.* **1953**, *75*, 38.
(5) Legters, J.; Thijs, L.; Zwanenburg, B. *Recl. Trav. Chim. Pays-Bas* **1992**, *111*, 75.
(6) Gentilucci, L.; Grijzen, Y.; Thijs, L.; Zwanenburg, B. *Tetrahedron Lett.* **1995**, *36*, 4665.
(7) Verstappen, M. M. H.; Ariaans, G. J. A.; Zwanenburg, B. *J. Am. Chem. Soc.* **1996**, *118*, 8491.
(8) Davis, F. A.; Liu, H.; Liang, C. H.; Reddy, G. V.; Zhang, Y. L.; Fang, T. N.; Titus, D. D. *J. Org. Chem.* **1999**, *64*, 8929.
(9) Davis, F. A.; Reddy, G. V.; Liu, H. *J. Am. Chem. Soc.* **1995**, *117*, 3651.
(10) Anderson, D. J.; Hassner, A. *Synthesis* **1975**, 483.
(11) Padwa, A.; Woolhouse, A. D. In *Comprehensive Heterocyclic Chemistry*; Katritzky, A. R., Rees, C. W., Eds.; Pergamon Press: Oxford, 1984; Vol. 7, pp 47−93.
(12) Nair, V. In *Heterocyclic Compounds*; Hassner, A., Ed.; John Wiley and Sons: New York, 1983; Vol. 42, Part I, pp 215−332.
(13) Palacios, F.; de Retana, A. M. O.; de Marigorta, E. M.; de los Santos, J. M. *Eur. J. Org. Chem.* **2001**, 2401.
(14) Palacios, F.; de Retana, A. M. O.; de Marigorta, E. M.; de los Santos, J. M. *Org. Prep. Proced. Int.* **2002**, *34*, 219.
(15) Gilchrist, T. L. *Aldrichimica Acta* **2001**, *34*, 51.
(16) Bucher, C. B.; Heimgartner, H. *Helv. Chim. Acta* **1996**, *79*, 1903.
(17) Padwa, A.; Dharan, M.; Smolanof, J.; Wetmore, S. I. *J. Am. Chem. Soc.* **1973**, *95*, 1954.
(18) Pinho e Melo, T. M. V. D.; Lopes, C. S. J.; Rocha Gonzalves, A. M. d'A.; Beja, A. M.; Paixão, J. A.; Silva, M. R.; da Veiga, L. A. *J. Org. Chem.* **2002**, *67*, 66.
(19) Palacios, F.; Ochoa de Retana, A. M.; Martínez de Marigota, E.; de los Santos, J. M. *Org. Prep. Proced. Int.* **2002**, *34*, 219.
(20) Tanner, D. *Angew. Chem., Int. Ed. Engl.* **1994**, *33*, 599.
(21) Righi, G.; D'Achille R.; Bonini C. *Tetrahedron. Lett.* **1996**, *37*, 6893.
(22) Lim, Y. H.; Lee, W. K. *Tetrahedron Lett.* **1995**, *36*, 8431.
(23) Tanner, D.; Birgersson, C.; Dhaliwal, H. K. *Tetrahedron. Lett.* **1990**, *31*, 1903.
(24) Lohr, L. L.; Hanamura, M.; Morokuma, K. *J. Am. Chem. Soc.* **1983**, *105*, 5541.
(25) Doughty, A.; Bacskay, G. B.; Mackie. J. C. *J. Phys. Chem.* **1994**, *98*, 13546.
(26) Pinho e Melo, T. M. V. D.; Lopes, C. S. J.; Rocha Gonsalves, A. M. d'A.; Storr, R. C. *Synthesis* **2002**, 605.
(27) Wendling, L. A.; Bergman, R. G. *J. Org. Chem.* **1976**, *41*, 831.
(28) Claus, P.; Doppler, T.; Gakis, N.; Georgarakis, M.; Giezendanner, H.; Gilgen, P.; Helmgartner, H.; Jackson, B.; Marky, M.; Narasimhan, N. S.; Rosenkranz, H. J.; Wunderli, A.; Hansen, H. J.; Schmid, H. *Pure Appl. Chem.* **1973**, *33*, 339.
(29) Padwa, A.; Dharan, M.; Smolanoff, J.; Wetmore, S. L., Jr. *Pure Appl. Chem.* **1973**, *33*, 269.
(30) Bigot, B.; Sevin, A.; Devaquet, A. *J. Am. Chem. Soc.* **1978**, *100*, 6924.
(31) Barcus, R. L.; Wright, B. B.; Platz, M. S.; Scaiano, J. C. *Tetrahedron Lett.* **1983**, *24*, 3955.
(32) Barcus, R. L.; Hadel, L. M.; Johnston, L. J.; Platz, M. S.; Savino, T. G.; Scaiano, J. C. *J. Am. Chem. Soc.* **1986**, *108*, 3928.

(33) Salem, L. *J. Am. Chem. Soc.* **1974**, *96*, 3486.
(34) Klessinger, M.; Bornemann, C. *J. Phys. Org. Chem.* **2002**, *15*, 514.
(35) Bornemann, C.; Klessinger, M. *Chem. Phys.* **2000**, *259*, 263,
(36) Albrecht, E.; Mattay, J.; Steenken, S. *J. Am. Chem. Soc.* **1997**, *119*, 11605.
(37) Whittle, E.; Dows, D. A.; Pimentel, G. C. *J. Chem. Phys.* **1954**, *22*, 1943.
(38) Frei, H.; Pimentel, G. C. In *Chemistry and Physics of Matrix-Isolated Species;* Andrews, L., Moskovits, M. Eds.; Elsevier Science Publishers: New York, 1989; Chapter 6, pp 139−166.
(39) Orton, E.; Collins, S. T.; Pimentel, G. C. *J. Phys. Chem.* **1986**, *90*, 6139.
(40) Collins, S. T.; Pimentel, G. C. *J. Phys. Chem.* **1984**, *88*, 4258.
(41) Inui, H.; Murata, S. *J. Am. Chem. Soc.* **2005**, *127*, 2628.
(42) Inui, H.; Murata, S. *Chem. Phys. Lett.* **2002**, *359*, 267.
(43) Inui, H.; Murata, S. *Chem. Lett.* **2001**, 832.
(44) Pinho e Melo, T. M. V. D.; Rocha Gonsalves, A. M. d'A.; Lopes, C. S. J.; Gilchrist, T. L. *Tetrahedron Lett.* **1999**, *40*, 789.
(45) Pinho e Melo, T. M. V. D.; Lopes, C. S. J.; Cardoso, A. L.; Rocha Gonsalves, A. M. d'A. *Tetrahedron* **2001**, *57*, 6203.
(46) Wasserman, H. H.; Ennis, D. S.; Blum, C. A.; Rotello, V. M. *Tetrahedron Lett*. **1992**, *33*, 6003.
(47) Frisch, M. J.; Trucks, G. W.; Schlegel, H. B.; Scuseria, G. E.; Robb, M. A.; Cheeseman, J. R.; Zakrzewski, V. G.; Montgomery, J. A., Jr.; Stratmann, R. E.; Burant, J. C.; Dapprich, S.; Millam, J. M.; Daniels, A. D.; Kudin, K. N.; Strain, M. C.; Farkas, O.; Tomasi, J.; Barone, V.; Cossi, M.; Cammi, R.; Mennucci, B.; Pomelli, C.; Adamo, C.; Clifford, S.; Ochterski, J.; Petersson, G. A.; Ayala, P. Y.; Cui, Q.; Morokuma, K.; Malick, D. K.; Rabuck, A. D.; Raghavachari, K.; Foresman, J. B.; Cioslowski, J.; Ortiz, J. V.; Stefanov, B. B.; Liu, G.; Liashenko, A.; Piskorz, P.; Komaromi, I.; Gomperts, R.; Martin, R. L.; Fox, D. J.; Keith, T.; Al-Laham, M. A.; Peng, C. Y.; Nanayakkara, A.; Gonzalez, C.; Challacombe, M.; Gill, P. M. W.; Johnson, B. G.; Chen, W.; Wong, M. W.; Andres, J. L.; Head-Gordon, M.; Replogle, E. S.; Pople, J. A. *Gaussian 98*, revision A.9; Gaussian, Inc.: Pittsburgh, PA, 1998.
(48) Frisch, M. J.; Trucks, G. W.; Schlegel, H. B.; Scuseria, G. E.; Robb, M. A.; Cheeseman, J. R.; Montgomery, J. A., Jr.; Vreven, T.; Kudin, K. N.; Burant, J. C.; Millam, J. M.; Iyengar, S. S.; Tomasi, J.; Barone, V.; Mennucci, B.; Cossi, M.; Scalmani, G.; Rega, N.; Petersson, G. A.; Nakatsuji, H.; Hada, M.; Ehara, M.; Toyota, K.; Fukuda, R.; Hasegawa, J.; Ishida, M.; Nakajima, T.; Honda, Y.; Kitao, O.; Nakai, H.; Klene, M.; Li, X.; Knox, J. E.; Hratchian, H. P.; Cross, J. B.; Bakken, V.; Adamo, C.; Jaramillo, J.; Gomperts, R.; Stratmann, R. E.; Yazyev, O.; Austin, A. J.; Cammi, R.; Pomelli, C.; Ochterski, J. W.; Ayala, P. Y.; Morokuma, K.; Voth, G. A.; Salvador, P.; Dannenberg, J. J.; Zakrzewski, V. G.; Dapprich, S.; Daniels, A. D.; Strain, M. C.; Farkas, O.; Malick, D. K.; Rabuck, A. D.; Raghavachari, K.; Foresman, J. B.; Ortiz, J. V.; Cui, Q.; Baboul, A. G.; Clifford, S.; Cioslowski, J.; Stefanov, B. B.; Liu, G.; Liashenko, A.; Piskorz, P.; Komaromi, I.; Martin, R. L.; Fox, D. J.; Keith, T.; Al-Laham, M. A.; Peng, C. Y.; Nanayakkara, A.; Challacombe, M.; Gill, P. M. W.; Johnson, B.; Chen, W.; Wong, M. W.; Gonzalez, C.; Pople, J. A. *Gaussian 03*, revision C.02; Gaussian, Inc.: Wallingford, CT, 2004.
(49) Becke, A. D. *Phys. Rev. A: At., Mol., Opt. Phys.* **1988**, *38*, 3098.
(50) Lee, C. T.; Yang, W. T.; Parr, R. G. *Phys. Rev. B: Condens. Matter Mater. Phys.* **1988**, *37*, 785.
(51) Csaszar, P.; Pulay, P. *J. Mol. Struct.* **1984**, *114*, 31.
(52) Farkas, O.; Schlegel, H. B. *J. Chem. Phys.* **1999**, *111*, 10806.
(53) Peng, C.; Schlegel, H. B. *Isr. J. Chem.* **1993**, *33*, 449.
(54) Schachtschneider, J. H. *Technical Report*; Shell Development Co.: Emeryville, CA, 1969.
(55) Wiberg, K. B.; Laidig, K. E. *J. Am. Chem. Soc.* **1987**, *109*, 5935.
(56) Teixeira-Dias, J. J. C.; Fausto, R. *J. Mol. Struct.* **1986**, *144*, 199.
(57) Lii, J.-H. *J. Phys. Chem. A* **2002**, *106*, 8667.
(58) Maçôas, E. M. S.; Khriachtchev, L.; Pettersson, M.; Fausto, R.; Räsänen, M. *J. Phys. Chem. A* **2005**, *109*, 3617.
(59) Barnes, A. *J. Mol. Struct.* **1984**, *113*, 161.
(60) Gómez Zavaglia, A.; Reva, I. D.; Fausto, R. *Phys. Chem. Chem. Phys.* **2003**, *5*, 41.
(61) Reva, I. D.; Stepanian, S. G.; Adamowicz, L.; Fausto, R. *Chem. Phys. Lett.* **2003**, *374*, 631.
(62) Borba, A.; Gómez-Zavaglia, A.; Simões, P. N. N. L.; Fausto, R. *J. Phys. Chem. A* **2005**, *109*, 3578.
(63) Gómez-Zavaglia, A.; Fausto, R. *Phys. Chem. Chem. Phys*. **2003**, *5*, 52.
(64) Abe, H.; Takeo, H.; Yamada, K. M. T. *Chem. Phys. Lett.* **1999**, *311*, 153.
(65) Lundell, J.; Krajewska, M.; Räsänen, M. *J. Phys. Chem. A* **1998**, *102*, 6643.
(66) Lopes, S.; Gómez-Zavaglia, A.; Lapinski, L.; Fausto, R. *J. Phys. Chem. A* **2005**, *109*, 5560.